Biochimica et Biophysica Acta 813 (1985) 253–265
Elsevier

BBA 72489

The effects of pressure and cholesterol on rotational motions of perylene in lipid bilayers

Parkson Lee-Gau Chong [a,b,*], B. Wieb van der Meer [a,**] and T.E. Thompson [b]

[a] *Departments of Biochemistry and Physics, University of Illinois, Urbana, IL 61801 and* [b] *Department of Biochemistry, University of Virginia, Charlottesville, VA 22908 (U.S.A.)*

(Received September 17th, 1984)

Key words: Phospholipid bilayer; Pressure; Cholesterol; Rotational motion; Perylene; Fluorescence polarization

Using steady-state fluorescence polarization measurements, an isothermal pressure-induced phase transition was observed in dimyristoyl-L-α-phosphatidylcholine multilamellar vesicles containing perylene. The temperature-to-pressure equivalence, dT/dP, estimated from the phase transition pressure, $P_{1/2}$, is about 22 K · kbar^{-1}, which is comparable to values determined from diphenylhexatriene polarization (Chong, P.L.-G. and Weber, G. (1983) Biochemistry 22, 5544–5550). In addition, we have employed a new method, introduced in this paper, to calculate the rate of in-plane rotation (R_{ip}) and the rate of out-of-plane rotation (R_{op}) of perylene in lipid bilayers. The effects of pressure and cholesterol on the rotational rates of perylene in two lipid bilayer systems have been examined. They are 1-palmitoyl-2-oleoyl-L-α-phosphatidylcholine (POPC) multilamellar vesicles (MLV) and 50 mol% cholesterol in POPC (MLV). R_{op} is smaller than R_{ip} due to the fact that the out-of-plane rotation requires a larger volume change than the in-plane rotation. Cholesterol seems not to affect R_{op} significantly, but pressure causes a decrease in R_{op} by about a factor of three. In contrast, the effects of pressure and cholesterol on R_{ip} are less straightforward. At 1 atm cholesterol increases R_{ip} by a factor of about two. Similarly, in the absence of cholesterol, 1.5 kbar pressure essentially triples R_{ip}. However, if both cholesterol is added and pressure is applied, R_{ip} decreases sharply. The possible interactions between cholesterol and perylene are discussed.

Introduction

Perylene is a flat aromatic molecule with a rigid, disk-like structure. Its diameter is about 8 Å. The structure is shown in Fig. 1, where the z-axis is chosen perpendicular to the ring system and the x-axis is along the emission dipole moment. The absorption moment lies also in the plane of the ring, at an angle α with respect to the x-axis. The fundamental anisotropy, r_0, which is the fluorescence anisotropy of the probe in the absence of rotation, measured at low temperatures in a very viscous solvent, depends on this angle only [1,2]:

$$r_0 = \frac{1+3\cos 2\alpha}{10} \quad (1)$$

In this paper we are concerned with perylene fluorescence in lipid bilayer systems. In such systems reorientations of an ensemble of excited probes occur during the fluorescence lifetime and, as a result the steady-state fluorescence anisot-

* Present address: Department of Biochemistry and the Biophysics Program, University of Virginia, Charlottesville, VA 22908, U.S.A.

** Present address: The Netherlands Cancer Institute, Plesmanlaan 121, NL-1066 CX Amsterdam, The Netherlands.

Abbreviations: DMPC, dimyristoyl-L-α-phosphatidylcholine; POPC, 1-palmitoyl-2-oleoyl-L-α-phosphatidylcholine; MLV, multilamellar vesicles.

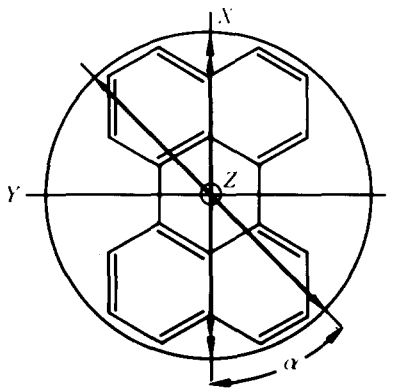

Fig. 1. The molecular structure of perylene showing the nearly cylindrical symmetry about the z-axis, perpendicular to the plane of the molecule. The absorption moment (↔) and emission moment (← →) are indicated. The angle α between absorption and emission moments varies with the excitation wavelength.

ropy, r, differs from r_0. Disk-like fluorophores embedded in the lipid bilayer have two principal modes of rotation: about the z-axis (in-plane) and about an axis located in the plane of the ring systems (out-of-plane), as indicated in Fig. 2. The

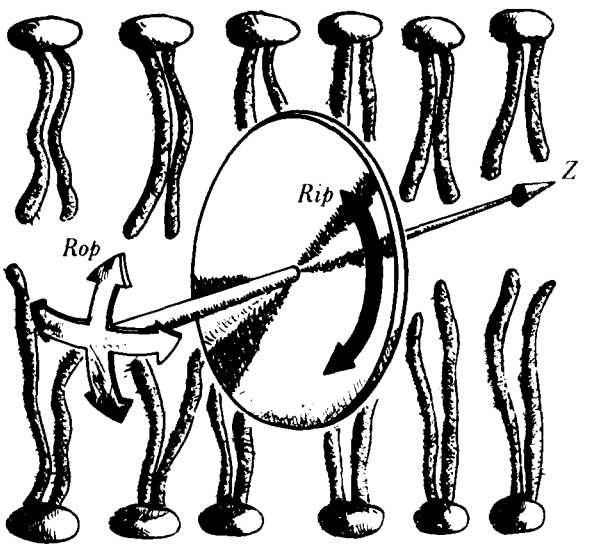

Fig. 2. Perylene with its nearly disk-like shape is shown aligned with the acyl chains of the lipids in its most probable orientation. The two distinct modes of reorientations are indicated; R_{ip} denotes the rate of the in-plane rotations and R_{op} that of the out-of-plane rotations.

rotational motion of perylene is anisotropic; the rate of the in-plane rotation (R_{ip}) is larger than the rate of the out-of-plane rotation (R_{op}) [3] and the rotational anisotropy ξ, defined as

$$\xi = \frac{R_{ip} - R_{op}}{R_{ip} + 2R_{op}} \tag{2}$$

is positive. The fluorescence anisotropy not only depends on the rotational rates, but also on the hindrance imposed by neighboring acyl chains in the bilayer. The reorientational order of the lipid acyl chain can be expressed in terms of the order parameter S:

$$S = \left\langle \frac{3\cos^2\theta - 1}{2} \right\rangle \tag{3}$$

where θ is the angle between the molecular z-axis and the bilayer normal, and the angular brackets denote an ensemble average. The X-Y plane of the rigid perylene molecule presumably aligns parallel to the acyl chains [2] (see Fig. 2), so that the most probable orientation of the neighboring acyl chains is at $\theta = 90°$ and a negative order parameter is thus expected [2]. The limiting fluorescence anisotropy, r_∞, which is essentially the steady-state anisotropy in the case of extremely rapid rotational motion, depends on the order parameter as follows [4,5]:

$$r_\infty = S^2/10 \tag{4}$$

Perylene has the interesting property which permits the angle between absorption and emission transition moments to be varied from 22° to 90° by appropriately choosing the excitation wavelength in the 270–410 nm range. In the present study we have employed this property to investigate the rotational motion of perylene embedded in multilamellar vesicles of 1-palmitoyl-2-oleoyl-L-α-phosphatidylcholine as a function of cholesterol concentration and pressure. The fundamental anisotropy has been obtained in a viscous solvent and the steady-state anisotropy and the fluorescence lifetime have been measured in the lipid bilayer system as a function of the excitation wavelength.

Various models have been proposed for analyzing such data:

(1) The slow rotation model [1,7,8], which yields

a simple expression relating the steady-state and the fundamental fluorescence anisotropies to the rotational rates of disk-like probes. The theory for this model has been derived by Weber [7] under the condition that the rates of rotational motion are small compared to the rate of emission.

(2) The anisotropic free rotor model [3,9], in which the anisotropy of the rotations is taken into account, but the hindrance is ignored.

(3) The isotropic hindered rotor model [1,3,10], which accounts for the hindrance, but ignores the rotational anisotropy.

Ideally, the rotational rates and orientations of perylene in lipid bilayers should come from dynamic data (time resolved or modulation frequency resolved). Such data are not available in the literature. The results reported in this paper indicate, however, that the rotational motion of perylene in lipid bilayers is fast, anisotropic and may be hindered. Therefore, none of these models is appropriate and a more general theory is needed. In this study we apply a recently reported theoretical analysis [2,4,5,6] to the steady-state fluorescence anisotropy of perylene and introduce a new method for evaluating the rates of in-plane and out-of-plane rotations of perylene in lipid bilayers.

Fluorescence depolarization theory for perylene

Here we introduce an approximate expression for the steady-state fluorescence anisotropy of perylene in lipid bilayers that accounts not only for the hindrance, but for the rotational anisotropy as well. It is derived in Appendix A from a more general treatment [5],

$$r = r_\infty + \frac{0.1 - r_\infty}{1+6R'\tau} + \frac{r_0 - 0.1}{1+6R\tau} \tag{5}$$

with

$$R = \tfrac{1}{3}R_{op} + \tfrac{2}{3}R_{ip} \tag{6}$$

and

$$R' = \frac{R_{op}}{1-10r_\infty} = \frac{(1-\xi)R}{(1-S^2)(1+\xi)} \tag{7}$$

where τ is the fluorescence lifetime.

This expression can yield the equations given by the three models mentioned above if the appropriate limitations are imposed:

(1) In the slow rotation model, Vincent et al. [1] have shown that Weber's expression [7] for the fluorescence anisotropy can be formulated as a linear relation between the parameters X and Y defined as:

$$X = \frac{10r_0 - 1}{5r_0 + 1} \tag{8}$$

$$Y = \frac{5r_0\left(\frac{r_0}{r} - 1\right)}{2\tau(5r_0+1)} \tag{9}$$

In Appendix B it is shown that Eqn. 5 reduces to their expression:

$$Y = R_{op} + R_{ip}X \tag{10}$$

if $R_{ip}\tau \ll 1$ and $R_{op}\tau \ll 1$. If $R_{ip}\tau$ and $R_{op}\tau$ are not small, the relation Y versus X is non-linear.

(2) The anisotropy derived for the free rotor model for disk-like probes [3,9] is obtained when $r_\infty = 0$ is substituted in Eqn. 5:

$$r = \frac{0.1}{1+6R_{op}\tau} + \frac{(r_0 - 0.1)}{(1+2R_{op}\tau + 4R_{ip}\tau)} \tag{11}$$

(3) The corresponding function derived for the isotropic hindered rotor model, is obtained by setting $R' = R$:

$$r = r_\infty + \frac{r_0 - r_\infty}{1+6R\tau} \tag{12}$$

In Fig. 3 the rotational anisotropy as a function of the average rotational rate, R, is plotted following the anisotropic free rotor model and the isotropic hindered rotor model. In each plot the two limiting functions are shown as well as one intermediate case. Note that the extreme cases are the same in both models. Complete hindrance is equivalent to complete anisotropy and no hindrance is equivalent to no anisotropy. Moreover, Fig. 3 suggests that in intermediate cases it may be quite difficult to discriminate between the two models. However, it is very likely that the order contribution, r_∞, for perylene is small. This is because perylene will presumably align with the acyl chains, so that a negative order parameter is

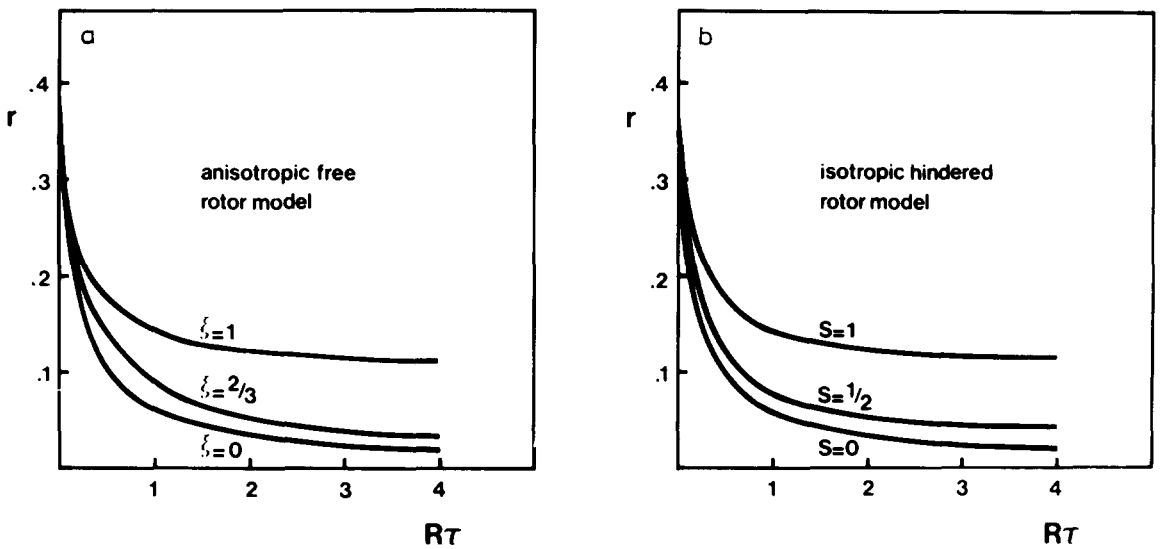

Fig. 3. The steady-state fluorescence anisotropy as a function of $R\tau$ in case of (a) the anisotropic free rotor model for various values of the rotational anisotropy ξ and in case of (b) the hindered isotropic rotor model for various values of the order parameter S. Symbols are defined in the text.

expected with $-1/2 \leq S \leq 0$ and $r_\infty \leq 1/40$. Therefore, the effect of rotational anisotropy will be dominant.

The graphical method of Lakowicz and Knutson [3] for determining R and r_∞ for the isotropic hindered rotor model can be extended to the general case given by Eqn. 5 as follows. By multiplying both sides of Eqn. 5 with $(1+6R\tau)/(6R\tau)$ and subtracting $r/(6R\tau)$ from both sides, Eqn. 5 transforms into:

$$r = r_i + \frac{r_0 - r}{6R\tau} \tag{13}$$

with

$$r_i = r_\infty + \frac{(0.1 - r_\infty)\left(1 - \frac{R'}{R}\right)}{1+6R'\tau}$$

$$= \frac{0.1[(1+\xi)(1-S^2)+(1-\xi)(S^2+6S^2R\tau-1)]}{(1+\xi)(1-S^2)+(1-\xi)6R\tau} \tag{14}$$

When the fundamental anisotropy, r_0, is varied by changing the excitation wavelength, a plot of the steady-state anisotropy, r, versus $(r_0 - r)/\tau$ will yield a straight line with slope equal to $1/(6R)$ and intercept equal to r_i, if the lifetime, τ, does not vary significantly with the excitation wavelength. Thus, R can be obtained and the allowed region in the ξ, S plane can be determined. The ξ, S plane is established by using Eqn. 14 with the calculated r_i and R values, and with the measured τ values for $-\frac{1}{2} \leq S \leq 0$. Next, the in-plane and out-of-plane rotational rates can be evaluated according to:

$$R_{ip} = \frac{(1+2\xi)R}{(1+\xi)} \tag{15}$$

$$R_{op} = \frac{(1-\xi)R}{(1+\xi)} \tag{16}$$

Eqns. 15 and 16 can be easily derived from Eqns. 2 and 6.

Materials and Methods

Materials. Dimyristoyl-L-α-phosphatidylcholine (DMPC) was obtained from Sigma. 1-Palmitoyl-2-oleoyl-L-α-phosphatidylcholine (POPC) was purchased from Avanti. Perylene and cholesterol were purchased from Aldrich Chemicals Co. and Steraloids, Inc., respectively.

Preparation of vesicles. Multilamellar vesicles (MLV) of DMPC, or POPC (with or without

cholesterol) were made by the method of Bangham et al. [11], as previously described [12]. Aliquots of perylene in ethanol were injected into the lipid dispersions, yielding a molar phosphatidylcholine/perylene ratio of about 100.

Fluorescence measurements. Fluorescence polarization was measured using a photon-counting polarization fluorometer [13]. Emission was observed through a Corning 3-72 filter in series with 2 mm of 1 M $NaNO_2$. In order to correct for the scattered light from vesicles, identical measurements were made on samples without perylene and these values were subtracted from the fluorescence intensities.

Fluorescence lifetimes were measured with the cross-correlation phase fluorometer designed by Spencer and Weber [14]. A light modulation frequency of 6 MHz was used for the measurements of lifetimes. The fluorescence lifetimes of perylene in vesicles were measured with respect to the scattered light from vesicles themselves. The scattered light served as the reference signal of zero phase delay. This was achieved by mounting a monochromator (H10 1200UV, Instruments SA Inc., Metuchen, NJ) at the emission side so that the appropriate wavelengths for the measurements of perylene fluorescence (448 nm was used) and for the measurements of scattered light (varied with the excitation wavelength) could be manually selected.

The procedures for the measurements of fluorescence lifetimes and polarization under pressure have been previously described [15,16]. The pressure vessel employed in this study was designed by Paladini and Weber [13].

Results

Pressure-induced phase transitions of DMPC multilamellar vesicles

The fluorescence anisotropy of perylene in dimyristoylphosphatidylcholine multilamellar vesicles was measured isothermally as a function of pressure at three temperatures. The results are shown in Fig. 4. The perylene fluorescence anisotropy was found to increase as the pressure increased. For each isothermal curve, an abrupt change in anisotropy is seen associated with the pressure-induced phase transition. The pressure dependence of perylene fluorescence anisotropy is almost completely reversible. A phase transition pressure, $P_{1/2}$, can be defined as the pressure at

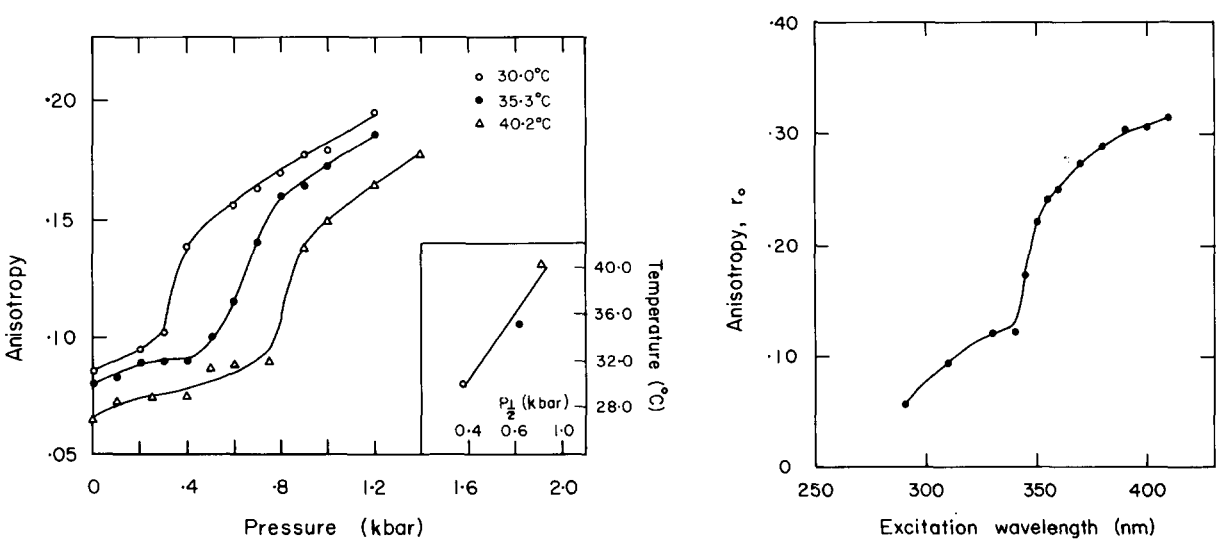

Fig. 4. Pressure dependence of perylene anisotropy in DMPC (multilamellar vesicles) at different temperatures. Excitation wavelength = 410 nm, emission filters: a 2 mm layer of 2 M $NaNO_2$ plus a Corning 3-72. Inset: Phase transition pressure, $P_{1/2}$, as a function of temperature.

Fig. 5. The anisotropy spectrum of perylene in glycerol at −13°C. Emission filters: a 2 mm layer of 2 M $NaNO_2$ plus a Corning 3-72.

which the abrupt increase in anisotropy is 50%. $P_{1/2}$ linearly changes with temperature, as shown in the inset of Fig. 4. This linearity is similar to that observed with diphenylhexatriene (Fig. 2 in Ref. 16). The slope of the $P_{1/2}$ versus temperature plot (inset, Fig. 4) gives a dT/dP value of 22 $K \cdot kbar^{-1}$, which is comparable to values reported elsewhere [12,15–19]. As shown in Table I, the values of $P_{1/2}$ determined from perylene polarization are very similar to those determined from diphenylhexatriene polarization for this system. These observations indicate that both probes are sensitive to the pressure-induced changes in the packing of lipid bilayers associated with the gel to liquid-crystalline phase transition.

Fundamental anisotropy spectrum of perylene

With the sample in the pressure bomb, the excitation anisotropy spectrum of perylene in glycerol was measured at −13°C. Under these conditions, the measured anisotropy is essentially the fundamental anisotropy, r_0, of the probe. The results, shown in Fig. 5, are very similar to those reported by Shinitzky et al. [8]. The values of r_0 shown in Fig. 5 were used for the subsequent calculations of R_{ip} and R_{op}.

Effects of pressure on perylene R_{ip} and R_{op} values in POPC vesicles and in (POPC + cholesterol) vesicles

The graphical method of Vincent et al. [1] was initially used to evaluate R_{ip} and R_{op} according to Weber's slow rotation model [7]. However, this method is clearly not appropriate for this system since R_{op} and R_{ip} are so large that the conditions that $R_{ip}\tau \ll 1$ and $R_{op}\tau \ll 1$ are not satisfied. This

TABLE I

PHASE TRANSITION PRESSURE, $P_{1/2}$, AS DETERMINED BY THE FLUORESCENCE POLARIZATION OF PERYLENE AND OF DIPHENYLHEXATRIENE (DPH) IN DMPC MULTILAMELLAR VESICLES

Temperature (°C)	$P_{1/2}$ (kbar)	
	Perylene	DPH [a]
30	0.38	0.31
35	0.59	0.51
40	0.82	0.77

[a] Data were obtained from Ref. 17.

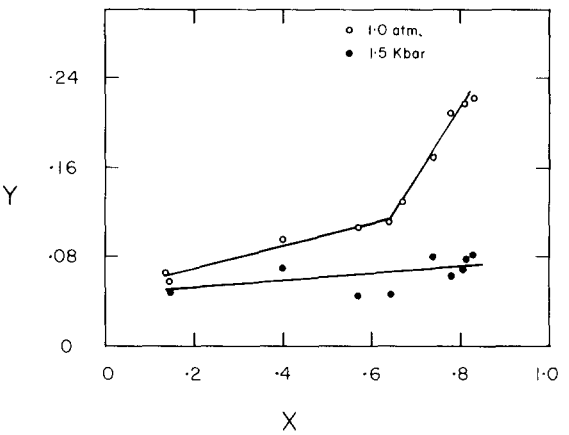

Fig. 6. Plot of Y vs. X for perylene in 50 mol% cholesterol in POPC at 10°C. Y and X are defined in Vincent et al. [1].

is evident not only from the values thus estimated, but from the non-linearity of the plot as shown in Fig. 6.

As an alternative we have plotted r versus $(r_0 - r)/\tau$. It is clear from inspection of Table II that the lifetimes vary slightly with excitation wavelength. However, since this variation is very small, the parameter r_i will be essentially constant and a plot of r versus $(r_0 - r)/\tau$ should yield a straight

TABLE II

THE FUNDAMENTAL ANISOTROPY, r_0, THE STEADY-STATE ANISOTROPY, r, AND THE PHASE-MEASURED LIFETIMES (MEASURED AT 6 MHz MODULATION FREQUENCY), $\tau(\phi)$, OF PERYLENE IN POPC WITHOUT AND WITH CHOLESTEROL (50 mol%) AT LOW (1 atm) AND HIGH (1.5 kbar) PRESSURE

A. Perylene in POPC without cholesterol at 1 atm and 10°C. Average $\tau = 5.99 \pm 0.42$ ns.

λ_{ex} (nm)	$\tau(\phi)$ (ns)	r_0	r	$(r_0 - r)/\tau$ (GHz)
410	4.47	0.3138	0.0725	0.054
400	5.23 [a]	0.3059	0.0768	0.044
390	6.38	0.3051	0.0619	0.038
380	6.05 [a]	0.2901	0.0633	0.037
370	5.71	0.2751	0.0711	0.036
350	6.06	0.2206	0.0506	0.028
345	6.70 [a]	0.1740	0.0478	0.019
340	7.34	0.1231	0.0387	0.011

[a] Interpolated values.

B. Perylene in POPC with 50 mol% cholesterol at 1 atm and 10°C. Average $\tau = 6.67 \pm 0.17$ ns.

λ_{ex} (nm)	$\tau(\phi)$ (ns)	r_0	r	$(r_0 - r)/\tau$ (GHz)
410	6.20	0.3138	0.0573	0.041
400	6.19	0.3059	0.0563	0.040
390	6.28	0.3051	0.0556	0.040
380	5.88	0.2901	0.0565	0.040
370	5.84	0.2751	0.0628	0.036
360	7.21	0.2514	0.0578	0.027
355	7.43	0.2405	0.0602	0.024
350	7.44	0.2206	0.0555	0.022
345	6.90	0.1739	0.0459	0.019
340	6.96	0.1231	0.0396	0.012
330	7.07	0.1217	0.0351	0.012

C. Perylene in POPC without cholesterol at 1.5 kbar and 10°C. Average $\tau = 5.87 \pm 0.44$ ns.

λ_{ex} (nm)	$\tau(\phi)$ (ns)	r_0	r	$(r_0 - r)/\tau$ (GHz)
410	5.01	0.3138	0.1003	0.043
390	6.30	0.3051	0.1021	0.032
370	5.87	0.2751	0.0913	0.031
350	4.73	0.2205	0.1073	0.024
330	7.46	0.1217	0.0849	0.005

D. Perylene in POPC with 50 mol% cholesterol at 1.5 kbar and 10°C. Average $\tau = 8.00 \pm 0.24$ ns.

λ_{ex} (nm)	$\tau(\phi)$ (ns)	r_0	r	$(r_0 - r)/\tau$ (GHz)
410	7.14	0.3138	0.1084	0.029
400	7.48	0.3059	0.1037	0.027
390	7.64	0.3051	0.1119	0.025
380	7.92	0.2901	0.1096	0.023
370	6.96	0.2751	0.0941	0.026
355	9.01	0.2405	0.0972	0.016
350	8.82	0.2206	0.0893	0.015
345	8.75	0.1739	0.0530	0.014
340	8.25	0.1231	0.0400	0.010

line according to Eqn. 13. This is shown in Fig. 7 for each of the four cases: 1 atm, 0 mol% cholesterol; 1 atm, 50 mol% cholesterol; 1.5 kbar, 0 mol% cholesterol and 1.5 kbar, 50 mol% cholesterol. The slope gives $R = (1/3)R_{op} + (2/3)R_{ip}$ and the intercept r_i depends on R, ξ and S. Results are presented in Table III. Note that the

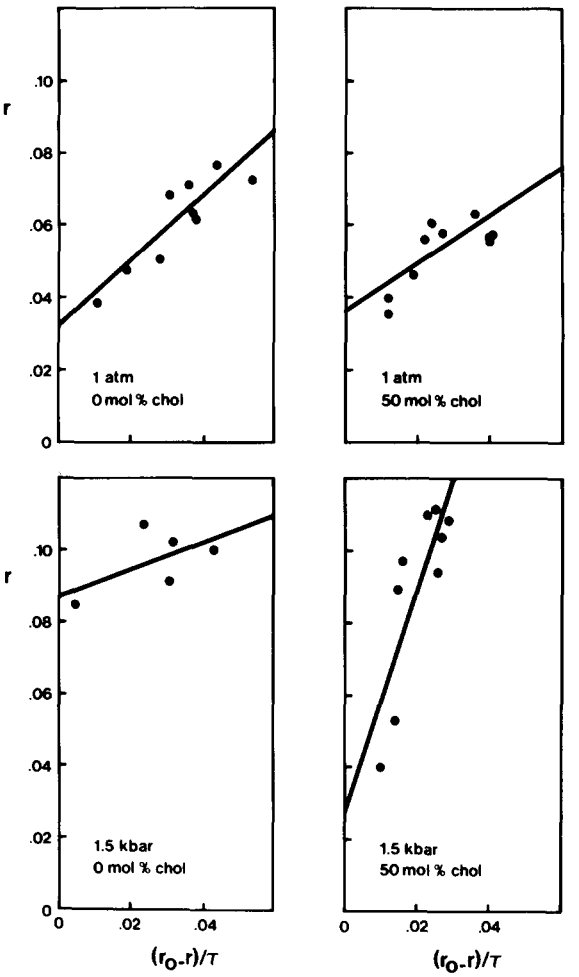

Fig. 7. The steady-state fluorescence anisotropy r as a function of $(r_0 - r)/\tau$ for perylene in POPC (multilamellar vesicles) at 10°C for the pressures and cholesterol concentrations indicated.

R values at 1 atm are close to those reported by Jacobson and Wobschall [20] who, however, used the Perrin equation to calculate the average rotational rate of perylene in egg phosphatidylcholine. Because the perylene molecules will preferentially align parallel to the acyl chains, the order parameter is expected to vary between 0 and $-\frac{1}{2}$. Consequently, the ranges for r_i and R presented in Table III correspond to allowed regions in the ξ, S plane. These are shown in Fig. 8. Using Eqns. 15 and 16, R_{ip} and R_{op} are determined. In Table IV, R_{ip} and R_{op} values are presented in the form of

$R_{ip} = \bar{R}_{ip} \pm \Delta R_{ip}$ and $R_{op} = \bar{R}_{op} \pm \Delta R_{op}$. The errors ($\Delta R_{ip}$ and ΔR_{op}) are estimated from the lower and upper limits of ξ and of R. For example, in the case of 0 mol% cholesterol at 1 atmosphere, we have used $R = 0.19 \pm 0.14$ (from Table III) and $\xi = 0.47 \pm 0.29$ (estimated from Fig. 8) to determine ΔR_{ip} and ΔR_{op}, by using the equations

$$\Delta R_{ip} = \left|\frac{\partial R_{ip}}{\partial \xi}\right| \Delta\xi + \left|\frac{\partial R_{ip}}{\partial R}\right| \Delta R$$

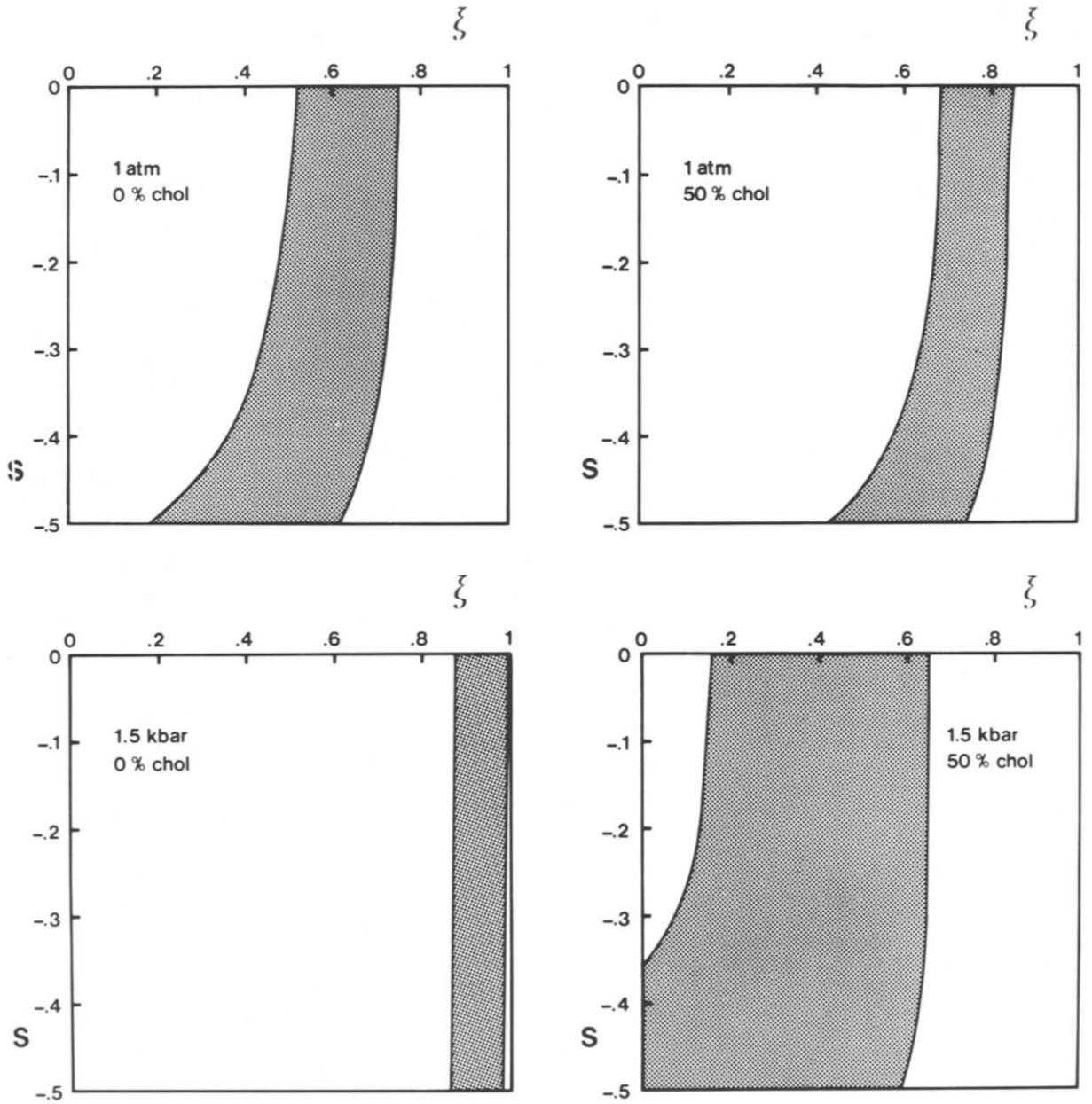

Fig. 8. The allowed regions in the ξ, S plane for the four cases that have been considered.

TABLE III

PARAMETERS OBTAINED FROM FITTING r VERSUS $(r_0 - r)/\tau$ (FIG. 7) TO A STRAIGHT LINE FOR PERYLENE IN POPC (MULTILAMELLAR VESICLES) AT 10°C FOR THE CASES: WITH AND WITHOUT CHOLESTEROL, AND AT LOW AND HIGH PRESSURE

A. $R = 1/3R_{op} + 2/3R_{ip}$ in GHz ($= 1/$ns)

Pressure	Cholesterol	
	None	50 mol%
1 atm	$R = 0.19 \pm 0.04$	$R = 0.29 \pm 0.08$
1.5 kbar	$R = 0.5 \pm 0.4$	$R = 0.0541 \pm 0.001$

B. The intercept r_i

Pressure	Cholesterol	
	None	50 mol%
1 atm	$r_i = 0.032 \pm 0.006$	$r_i = 0.036 \pm 0.005$
1.5 kbar	$r_i = 0.087 \pm 0.009$	$r_i = 0.03 \pm 0.02$

and

$$\Delta R_{op} = \left|\frac{\partial R_{op}}{\partial \xi}\right| \Delta\xi + \left|\frac{\partial R_{op}}{\partial R}\right| \Delta R$$

$\overline{R}_{ip}$ is the average of $R_{ip,min}$ and $R_{ip,max}$, with the relations that

$$R_{ip,min} = \frac{(1+2\xi_{min})R_{min}}{(1+\xi_{min})}$$

TABLE IV

THE EFFECTS OF PRESSURE AND CHOLESTEROL ON THE ROTATIONAL RATES OF PERYLENE IN POPC (MULTILAMELLAR VESICLES) AT 10°C

A. The rate of out-of-plane rotations, R_{op} in GHz ($= 1/$ns)

Pressure	Cholesterol	
	None	50 mol%
1 atm	$R_{op} = 0.09 \pm 0.07$	$R_{op} = 0.09 \pm 0.07$
1.5 kbar	$R_{ip} = 0.03 \pm 0.03$	$R_{op} = 0.03 \pm 0.02$

B. The rate of in-plane rotations, R_{ip} in GHz ($= 1/$ns)

Pressure	Cholesterol	
	None	50 mol%
1 atm	$R_{ip} = 0.25 \pm 0.08$	$R_{ip} = 0.41 \pm 0.14$
1.5 kbar	$R_{ip} = 0.75 \pm 0.60$	$R_{ip} = 0.06 \pm 0.02$

and

$$R_{ip,max} = \frac{(1+2\xi_{max})R_{max}}{(1+\xi_{max})}$$

In the case of $\overline{R}_{op}$

$$R_{op,min} = \frac{(1-\xi_{max})R_{min}}{(1+\xi_{max})}$$

and

$$R_{op,max} = \frac{(1-\xi_{min})R_{max}}{(1+\xi_{min})}$$

Discussion

Pressure-induced gel to liquid crystalline phase transitions in DMPC vesicles can be readily observed by measuring the fluorescence anisotropy of perylene embedded in the lipid bilayer (Fig. 4). At a given temperature, the value of $P_{1/2}$ (Table I) determined from perylene polarization as equal to $3r/(2+r)$ (r = fluorescence anisotropy) is close to that determined from diphenylhexatriene polarization [17]. In addition, the dT/dP value determined from the inset of Fig. 4 is in good agreement with that determined from the diphenylhexatriene study in the DMPC multilamellar vesicles [16]. These observations suggest that perylene as well as diphenylhexatriene can be used as a probe to monitor the pressure-induced phase transition in lipid bilayers and that the observed pressure effects on phase transitions are probe independent.

Although diphenylhexatriene and perylene give similar measures of pressure-induced phase transitions, the rotational motions of these two probes in vesicles must be quite different because of the different shapes of the two probe molecules. In order to study the probe rotational motions in vesicles, a relation between the dynamic behavior and the steady-state anisotropy is needed. For diphenylhexatriene, such a relation is well established (Ref. 21 and references cited therein); for perylene, on the other hand, this has not been the case. Eqns. 5–16 derived in this paper describe the relation between the steady-state anisotropy of perylene and its dynamic behavior (rotational

rates) as well as the rotational hindrance and the rotational anisotropy.

Although hindrance and rotational anisotropy can have similar effects on perylene fluorescence anisotropy, as shown in Fig. 3 the factor S^2 in Eqn. 4 is likely not to exceed 0.25, and thus the hindrance contribution probably is of minor importance. This is the case because the preferred orientation of the X-Y plane of perylene is parallel to the long axes of the lipid acyl chains. In this respect perylene is distinctly different from diphenylhexatriene. The fluorescence anisotropy of diphenylhexatriene is so sensitive to the molecular order, that it is misleading to interpret the fluorescence anisotropy of diphenylhexatriene in terms of a microviscosity [21]. Perylene fluorescence anisotropy in lipid bilayers, on the other hand, seems not to be influenced greatly by the order parameter, but it is sensitive to variations in the rotational rates and thus also in the rotational anisotropy ξ. This conclusion is quite different from that made by Lakowicz and Knutson [3], who state that the steady-state anisotropy of perylene in lipid bilayers is representative of r_∞ and not of the Brownian rotational rate. However, while predicting that apparent r_∞ values do not exceed 0.1 [3], they report values larger than 0.1 on some occasions (Fig. 7 in Ref. 3). These discrepancies may be due to their neglect of the rotational anisotropy ξ or due to the possibility that the shape of perylene is not exactly a disk, so that the approximation of R_{op} (about x-axis) = R_{op} (about y-axis) is not completely justified.

A complication may arise if a fraction of the probe is orientated parallel to the membrane plane and the remaining is perpendicular, because a different probe distribution would yield a different molecular order parameter. In fact, such a distribution has been suggested for diphenylhexatriene in lipid bilayers above the transition temperature [22]. In principle, this possibility could be examined for perylene, if the fourth rank order parameter were taken into account in time-resolved measurements [5,6,22]. This parameter was not considered in this study, however. To do so would have required more sophisticated equipment than is currently available to us.

The values of R_{op} and R_{ip} obtained under several conditions are listed in Table IV. The values of R_{op} are small and equal for both the cholesterol-free and the 50 mol% cholesterol systems. An increase in pressure from 1 atm to 1.5 kbar decreases R_{op} in both systems by a factor of 3. Out-of-plane rotations require a substantial local free volume. The small values of R_{op} reflect the infrequent occurrences of sufficient free volume in the locality of the probe. The decrease in R_{op} with an increase in pressure almost certainly reflects a decrease in free volume accompanying the pressure increase.

Table IV shows the values of R_{ip} to be substantially larger than the values of R_{op} under similar conditions. This most probably reflects the relatively small free volume requirement for in-plane rotations relative to out-of-plane rotations. However, the variation of R_{ip} with pressure in the two systems is complicated. In the pure POPC system R_{ip} increases with increasing pressure while in the 50 mol% cholesterol system it decreases with increasing pressure as did R_{op}. The result can be explained as follows.

In general three factors are expected to effect the rotational rate: hindrance, rotational mode and the local free volume. As discussed above, the hindrance contribution is probably of minor importance because of the small values of S^2. The free volume decrease should cause R_{ip} to decrease not increase. It therefore seems plausible that the observed increase in R_{ip} is due to a change in rotational mode. The Brownian rotation of small molecules depends on the interactions between the solvent molecules (POPC and/or cholesterol in our case) and the surface of the probe molecule (perylene). Two types of interaction conditions giving rise to two rotational modes have been proposed [23]. Under sticking boundary conditions, the solvent molecules move with the probe molecule and the rotations of the probe molecules are strongly damped [23,24]. Under slipping boundary conditions, the rotations of the probe molecule are essentially without frictional force [23]. It is known that the rotation with the slipping boundary conditions is faster than that with the sticking boundary conditions [23]. It is possible that the increase in R_{ip} with increasing pressure in the case of POPC (Table IV) is due to a weighted change in rotational mode from 'sticking' to 'slipping' when the pressure is raised to 1.5 kbar. The

basis for this suggestion is the fact that the acyl chains become more rigid and thus less entangled with perylene at 1.5 kbar. This explanation has been involved previously to explain an increase in the rotation rate of diphenylhexatriene with a combined increase in pressure and a decrease in temperature in a biological membrane [15]. This concept has also been used in other studies of the rotational motions of small molecules [24–26]. The 'sticking-slipping' mode change would have no effect on R_{op}, because the values of R_{op}(slip)/R_{op}(stick) for very flattened oblate ellipsoids (such as perylene) are near unity as shown by Hu and Zwanzig [23].

In the case of 50 mol% cholesterol in POPC, the rotational mode change is probably less important in determining R_{ip}. This is because the tetracyclic ring of cholesterol has a flat underface and is rigid [27]. As a result, cholesterol molecules do not readily stick on perylene even at atmospheric pressure. In this case, a weighted change in the rotational mode in response to the pressure perturbation may not occur or occurs to a much lesser extent. Because of this, the volume effect, instead of the rotational mode, becomes dominating. Consequently, R_{ip} drops as the pressure increases.

50 mol% cholesterol in POPC is a more complex system than pure POPC. In addition to the rotational mode and the volume effects, the possible relocation of probe molecules between the cholesterol-enriched domains and the phospholipid-enriched domains must be taken into consideration. In the absence of information about the pressure dependence of probe partitioning, a full discussion on the effect of probe relocation on R_{ip} and R_{op} is not possible at present. However, important to the subject of this paper is the fact that the lipids in biological membranes have interactions with many other membrane components. If cholesterol does indeed provide a less sticky environment for perylene, cholesterol might then modulate the interactions between membrane lipids and other membrane components.

Conclusions

We have presented a new method by which the individual rotational rates of a disk-like molecule can be calculated. Applications of this method demonstrates the following:

(1) Cholesterol does not influence the out-of-plane rotations of perylene in POPC (multilamellar vesicles) significantly.

(2) Pressure causes a decrease in the rate of the out-of-plane rotation.

(3) Cholesterol increases the rate of the in-plane rotation at atmospheric pressure, but causes a decrease at 1.5 kbar.

(4) Pressure enhances the in-plane rotation in the absence of cholesterol, but decreases it if cholesterol is present at a concentration of 50 mol%.

(5) Although a complete understanding of the effect of cholesterol and pressure on the rate of the in-plane rotation is not possible at present, it is quite clear from Table IV that the effects of hydrostatic pressure and cholesterol on R_{ip} and R_{op} of perylene in lipid bilayers are distinctly different.

Acknowledgements

This work was supported by a grant from the National Institutes of Health (GM11223) to Dr. Gregorio Weber and by a grant from the National Institutes of Health (GM14628) to Dr. Thomas E. Thompson. We thank Dr. G. Weber for use of his instruments and for helpful discussion, and to Drs. Ching-hsien Huang and W.J. Van Blitterswijk for stimulating discussion. B. Wieb van der Meer is grateful to the Netherlands Cancer Foundation for financial support, and to Drs. Enrico Gratton and Michael Glaser for their hospitality.

Appendix A

Derivation of the steady-state fluorescence anisotropy for perylene in a lipid bilayer

An expression for the fluorescence anisotropy of a cylindrically symmetric probe excited at time zero with a short flash of light, has been derived by Zannoni et al. (Eqn. 4.78b in Ref. 2) and by Van der Meer et al. (Eqn. 5 in Ref. 5). This can be applied to perylene simply by taking the angles between the molecular z-axis and the absorption and emission moments equal to 90°, yielding

$$r(t) = 0.1G_0(t) + 0.3 \cos 2\alpha G_2(t) \quad \text{(A1)}$$

where r is the fluorescence anisotropy, t is the time, α is the angle between absorption and emission moments and G_0 and G_2 denote time-dependent correlation functions. Here we follow the simplest approximation for the correlation functions by Van der Meer et al. (Eqn. 8 in Ref. 5), in which $G_0(t)$ and $G_2(t)$ are approximated by single exponentials plus a constant, such that they are exact for both short and long times. These functions read in that case

$$G_0(t) = S^2 + (1 - S^2)\exp\left(-6R_{op}t/(1 - S^2)\right) \tag{A2}$$

$$G_2(t) = \exp\left(-2R_{op}t - 4R_{ip}t\right) \tag{A3}$$

where R_{op} and R_{ip} are components of the rotational diffusion tensor of the probe; R_{op} is the average diffusion coefficient for the wobbling motion of the symmetry axis (i.e. z-axis) (the rate of out-of-plane rotations) and R_{ip} is the average diffusion coefficient for reorientations around this axis (the rate of in-plane rotations). The order parameter S is defined in Eqn. 3. It follows that the r at long times, the limiting fluorescence anisotropy equals

$$r_\infty = \frac{S^2}{10} \tag{A4}$$

and the r at zero time, the fundamental fluorescence anisotropy, is

$$r_0 = 0.1 + 0.3\cos 2\alpha \tag{A5}$$

The steady-state fluorescence anisotropy can be calculated as the time average of $r(t)$, weighted by the decay of the intensity:

$$r = \frac{\int_0^\infty r(t)\exp\left(-\frac{t}{\tau}\right)dt}{\int_0^\infty \exp\left(-\frac{t}{\tau}\right)dt}$$

$$= r_\infty + \frac{0.1 - r_\infty}{1 + \left(6R_{op}\tau/(1 - S^2)\right)} + \frac{r_0 - 0.1}{1 + 6R\tau} \tag{A6}$$

where τ is the fluorescence lifetime, $R = \frac{1}{3}R_{op} + \frac{2}{3}R_{ip}$ and Eqns. A4 and A5 have been used.

It should be noted that Lipari and Szabo [4] have provided an alternative expression for $G_2(t)$, which is more complicated in that it is a double exponential, but has the correct limit for $S \to 1$. In our approximation for $G_2(t)$ (Eqn. A3), it must be assumed that $R_{op} \to 0$ for $S \to 1$. However, in the present study S^2 is small, so that our approximation and that of Lipari and Szabo [4] lead to essentially the same results.

Appendix B

The X-Y relation

Eqn. 5 can be rewritten as

$$\frac{5r_0}{2\tau}\left(\frac{r_0}{r} - 1\right) = \frac{R_{op}(5r_0 + 1) + R_{ip}(10r_0 - 1) + 3R_{op}\left(R_{op} + 2R_{ip}\right)\tau(r_0 - r_\infty)/(0.1 - r_\infty)}{1 + \left\{3R_{op}\tau(r_0 + r_\infty - 0.1) + \left(R_{op}\tau + 2R_{ip}\tau\right)(0.1 - r_\infty + 6R_{op}\tau r_\infty)\right\}\left\{5r_0(0.1 - r_\infty)\right\}} \tag{B1}$$

After dividing by $(5r_0 + 1)$ and substituting Eqn. 9 into the lefthand side of Eqn. B1, and substituting Eqn. 8 and $r_0 = (1 + X)/(10 - 5X)$, which follows from Eqn. 8, into the righthand side of Eqn. B1, this expression becomes

$$Y = \frac{R_{op} + R_{ip}X + 2R_{op}\left(R_{op}\tau + 2R_{ip}\tau\right)\left\{1 + X(1 + 5r_\infty)/(1 - 10r_\infty)\right\}}{1 + 6R_{op}\tau/(1 - 10r_\infty) + 2(2 - X)\left(R_{ip}\tau - R_{op}\tau\right)/(1 + X) + 6(2 - X)R_{op}\tau\left(R_{op}\tau + 2R_{ip}\tau\right)(10r_\infty)/\left\{(1 + X)(1 - 10r_\infty)\right\}} \tag{B2}$$

If $R_{op}\tau \ll 1$ and $R_{ip}\tau \ll 1$ this equation reduces to Eqn. 10, but if $R_{ip}\tau$ and $R_{op}\tau$ are not small Y is clearly a nonlinear function of X.

References

1 Vincent, M., De Foresta, B., Galley, J. and Alfsen, A. (1982) Biochemistry 21, 708–716
2 Zannoni, C., Arcioni, A. and Cavatorta, P. (1983) Chem. Phys. Lipids 32, 179–250
3 Lakowicz, J. and Knutson, J.R. (1980) Biochemistry 19, 905–911
4 Lipari, G. and Szabo, A. (1980) Biophys. J. 30, 489–506
5 Van der Meer, W., Pottel, H., Herreman, W., Ameloot, M., Hendrickx, H. and Schröder, H. (1984) Biophys. J. 46, 515–523
6 Szabo, A. (1984) J. Chem. Phys. 81, 150–167
7 Weber, G. (1971) J. Chem. Phys. 55, 2399–2407
8 Shinitzky, M., Dianoux, A.-C., Gitler, C. and Weber, G. (1971) Biochemistry 10, 2106–2113
9 Tao, T. (1969) Biopolymers 8, 609–632
10 Kinosita, K., Kawato, S. and Ikegami, A. (1977) Biophys. J. 20, 289–305
11 Bangham, A.D., De Gier, J. and Greville, G.D. (1967) Chem. Phys. Lipids 1, 225–246
12 Chong, P.L.-G. and Cossins, A.R. (1984) Biochim. Biophys. Acta 772, 197–201
13 Paladini, A.A. and Weber, G. (1981) Rev. Sci. Instrum. 52, 419–427
14 Spencer, R.D. and Weber, G. (1969) Ann. N.Y. Acad. Sci. 158, 361–376
15 Chong, P.L.-G., Cossins, A.R. and Weber, G. (1983) Biochemistry 22, 409–415
16 Chong, P.L.-G. and Weber, G. (1983) Biochemistry 22, 5544–5550
17 Chong, P.L.-G. (1982) Ph.D. Dissertation, University of Illinois at Champaign-Urbana
18 Heremans, K. (1980) Rev. Phys. Chem. Jap. 50, 259–273
19 Wann, K.T. and MacDonald, A.G. (1980) Comp. Biochem. Physiol. A66A, 1–12
20 Jacobson, K. and Wobschall, D. (1974) Chem. Phys. Lipids 12, 117–131
21 Pottel, H., Van der Meer, W. and Herreman, W. (1983) Biochim. Biophys. Acta 730, 181–186
22 Ameloot, M., Hendrickx, H., Herreman, W., Pottel, H., Van Cauwelaert, F. and Van der Meer, W. (1984) Biophys. J. 46, 525–539
23 Hu, C.-M. and Zwanzig, R. (1974) J. Chem. Phys. 60, 4354–4357
24 Barkley, M.D., Kowalczky, A.A. and Brand, L. (1981) J. Chem. Phys. 75, 3581–3593
25 Mantulin, W.W. and Weber, G. (1977) J. Chem. Phys. 66, 169–176
26 Lepock, J.R., Cheng, K.-H., Campbell, S.D. and Kruuv, J. (1983) Biophys. J. 44, 405–412
27 Huang, C. and Mason, J.T. (1982) in Membranes and Transport, Vol. 1 (Martonosi, A.N., ed.), pp. 14–23, Plenum Publishing, New York